SAFE-LAND

Mitigating the risk of flooding and landslides via artificial intelligence with a view to extreme climate events

Deliverable 5.1:
Hydrogeological risk management: guidelines

Mitigating the risk of flooding and landslides via artificial intelligence with a view to extreme climate events

Co-funded by the
European Union

e-CAMPUS UNIVERSITÀ
UNIVERSITÀ DI PISA
MEĐIMURSKA ŽUPANIJA

Deliverable Title	Hydrogeological risk management: guidelines
Deliverable number	5.1
Deliverable Lead	UNIPI
Related Work Package	WP5: Trustworthy AI models: risk awareness
Author(s)	Francesco Pistolesi (UNIPI), Michele Baldassini (UNIPI), Matteo Mugnai (UNIPI), Marco Avvenuti (UNIPI), Nicola Tonellotto (UNIPI), Francesco Marcelloni (UNIPI)
Dissemination Level	Public
Due Submission Date	11/11/25
Actual Submission	12/04/25
Project Number	101140345
Status	Version 1.0 (12/04/25)
Reviewed (Authors)	Elisabetta Cattoni (eCampus), Francesco Focacci (eCampus)
Start Date of Project	12 February 2024
Duration	24 months
Abstract	This document is the Deliverable 4.2 of the project *"Mitigating the risk of flooding and landslides via artificial intelligence with a view to extreme climate events (SAFE-LAND)"*. The deliverable describes how hydrogeological guidelines are selected and tailored using the results obtained by the hydrogeological AI-based models.
Status changes history	Version 1.0 (12/04/2025) — First release

Funded by the European Union. Views and opinions expressed are however those of the author(s) only and do not necessarily reflect those of the European Union. Neither the European Union nor the granting authority can be held responsible for them.

Table of Contents

Funded by the European Union. Views and opinions expressed are however those of the author(s) only and do not necessarily reflect those of the European Union. Neither the European Union nor the granting authority can be held responsible for them.

1. Introduction

Hydrogeological hazards such as landslides, floods, debris flows, and surface runoff-induced erosion represent a significant threat to infrastructure and human safety in many European regions. Climate change amplifies these risks by increasing the frequency and intensity of extreme weather events, thus intensifying rainfall extremes, accelerating infiltration processes, and triggering rapid slope instabilities. In this evolving context, effective risk mitigation requires decision-support tools capable of integrating heterogeneous sources of information, handling uncertainty, and producing transparent, explainable, and spatially adaptive recommendations. The SAFE-LAND project addresses this challenge by developing an AI-driven framework that supports authorities and practitioners in identifying, evaluating, and prioritizing hydrogeological risk mitigation measures.

This deliverable describes how the guidelines by experts are tailored using artificial intelligence for geotechnical and hydraulic mitigation actions.

A central component of the SAFE-LAND system is a fuzzy logic decision-support model, designed to adapt qualitative expert assessments to a quantitative methodology that can be tailored to various scenarios. Traditional guideline tables classify mitigation measures according to discrete categories, such as "shallow" vs. "deep" sliding surfaces or "low" vs. "high" pore-water pressure. However, natural systems do not change sharply, and engineers frequently reason in terms of gradients rather than strict boundaries. Fuzzy logic captures this nuance by modeling hydrogeological variables through linguistic categories with gradual transitions. This allows the system to reflect the inherent uncertainty and variability of real slopes. The resulting Mamdani-type inference engine produces continuous effectiveness surfaces for each guideline and yields *objective*, *reproducible* rankings *adapted to site-specific conditions*.

Complementing the geotechnical perspective, SAFE-LAND incorporates a hydraulic hazard assessment module based on physically based simulations and machine-learning semantic segmentation. This module evaluates the water depth, arrival time, and flow velocity to classify terrain into actionable hazard categories (colored in green, yellow, orange, and red) as illustrated in the maps and diagrams throughout the document. These classifications support the identification of hydraulic mitigation guidelines targeting surface water management, energy dissipation, erosion control, and rapid-onset flood response.

By combining fuzzy geotechnical inference with high-resolution hydraulic hazard mapping, the integrated SAFE-LAND framework thus provides a multi-layered approach to risk mitigation that is both robust and operationally useful. The system bridges expert knowledge, AI-based prediction, and physical modeling to provide customized recommendations that can be adapted to complex hydrogeological realities. With this introduction we outlined the motivation and conceptual foundations behind the methodology detailed in the following sections.

2. Background

Fuzzy Logic, first introduced by Zadeh in 1965, constitutes a mathematical paradigm for representing, formalizing, and manipulating uncertain, vague, or linguistically described information. It emerged from the recognition that many real-world systems—in particular, those involving human reasoning, natural language, and environmental

Funded by the European Union. Views and opinions expressed are however those of the author(s) only and do not necessarily reflect those of the European Union. Neither the European Union nor the granting authority can be held responsible for them.

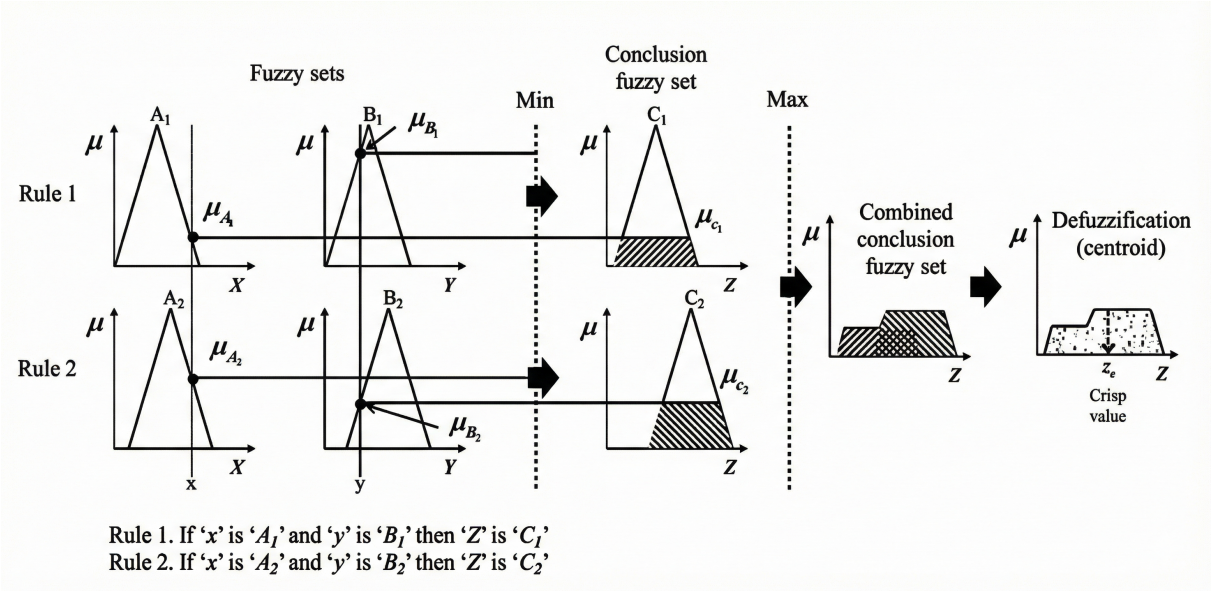

Fig. 1: A fuzzy inference system with two rules involving four fuzzy sets (A_1, B_1, A_2, and B_2). Membership functions are triangular and $\mu_{A_1}, \mu_{B_1}, \mu_{A_2}$, and μ_{B_2} quantify the membership degrees.

processes—cannot be adequately described using the rigid, binary structure of classical Boolean logic. In Boolean systems, a variable must belong entirely to a category or not belong to it at all (e.g. a state can only be "true" or "false", a condition can only be "safe" or "unsafe"). This dichotomous representation is incompatible with the way engineers, geologists, and domain experts conceptualize complex natural phenomena.

In contrast, fuzzy logic introduces the notion of *partial membership*, according to which an element may simultaneously belong to multiple sets with varying degrees of truth. For example, the statement "the sliding surface is deep" can hold true to a degree of 0.7, whereas the statement "the sliding surface is medium-depth" may also hold true to a degree of 0.4. This flexibility enables fuzzy logic to mirror the gradient-based reasoning characteristic of human expertise, capturing nuances that would otherwise be lost in a classical modeling approach.

Fuzzy logic is particularly useful when dealing with geotechnical and hydrogeological processes. For example, in slope stability analysis, input variables such as the "depth of the sliding surface", the "degree of saturation", or the "piezometric pressure" rarely exhibit discrete jumps between categories. In natural slopes, transitions between shallow, medium, and deep sliding conditions occur gradually, due to continuous geological and hydrological processes. Similarly, water table fluctuations do not instantaneously shift from "low" to "high", but evolve progressively in response to rainfall infiltration, drainage, and subsurface flow dynamics.

Expert terminology used in technical guidelines (e.g., *shallow*, *moderate*, *very deep*) implicitly acknowledges these gradual transitions. However, when these qualitative descriptors are translated into numerical models, there is a risk of losing this semantic richness. Fuzzy logic bridges this gap by allowing qualitative expert knowledge to be expressed using linguistic variables while preserving numerical interpretability and computational rigor. For these reasons, a fuzzy inference system (FIS) can be a suitable and powerful tool to link qualitative geotechnical assessments with quantitative predictive

Funded by the European Union. Views and opinions expressed are however those of the author(s) only and do not necessarily reflect those of the European Union. Neither the European Union nor the granting authority can be held responsible for them.

modeling.

Among the various FIS architectures, the *Mamdani-type* system we adopted is one of the most accurate and widely used approaches in the engineering of decision-support systems. This popularity comes from its interpretability, intuitive rule structure, and ability to directly encode expert knowledge in the form of logical statements. Rules of the type

$$\text{IF } (z_s \text{ is shallow}) \text{ AND } (z_w^{final} \text{ is high}) \text{ THEN effectiveness is low}$$

are immediately understandable by practitioners and can be directly validated against expert judgment.

The Mamdani fuzzy inference process comprises three main stages (see Fig. 1):

1. **Fuzzification**. Numerical inputs are mapped into fuzzy membership degrees through membership functions that quantify linguistic concepts. For example, a sliding surface depth of $z_s = 3$ m may simultaneously activate the *shallow* and *medium* with different membership degrees. This ensures that borderline conditions are represented more faithfully than in threshold-based systems.

2. **Rule evaluation and aggregation**. The fuzzified inputs are fed into a set of IF–THEN rules derived from expert knowledge and technical guidelines. Each rule contributes a fuzzy output according to the degree to which its antecedent conditions are satisfied. Multiple active rules are aggregated using fuzzy operators (typically the *minimum operator* for logical AND, and *maximum operator* for union) to produce a combined output fuzzy set. This stage mimics the process by which human experts synthesize multiple lines of reasoning under uncertainty.

3. **Defuzzification**. The aggregated fuzzy output, which represents effectiveness in linguistic terms (e.g. "medium", "high"), is converted into a numerical score through an appropriate defuzzification method. The centroid method, adopted in this study, computes the center of gravity of the aggregated fuzzy set, producing a balanced and physically interpretable scalar value. This value represents the estimated effectiveness of a mitigation guideline under specified hydrogeological conditions.

With these steps, the fuzzy system produces tailored, explainable, and continuous evaluations of guideline effectiveness, even when the underlying conditions are uncertain, partially known, or inherently imprecise. By combining linguistically expressed expert knowledge with mathematically rigorous inference mechanisms, the fuzzy logic approach offers a flexible and transparent decision-support tool that is particularly suited to the multi-parameter, uncertainty-rich context of landslide hazard mitigation.

3. Tailoring guidelines

This section presents the methodology developed to tailor structural and non-structural mitigation guidelines to site-specific hydrogeological conditions.

After introducing the principles of fuzzy logic and the rationale for its use in modeling uncertain or linguistically described information, we illustrate how these concepts are adapted in the context of landslide hazard mitigation.

Funded by the European Union. Views and opinions expressed are however those of the author(s) only and do not necessarily reflect those of the European Union. Neither the European Union nor the granting authority can be held responsible for them.

The procedure aims to translate expert-based guideline tables into a quantitative, continuous, and spatially adaptable decision-support system. This transformation is crucial as the original guideline frameworks—although grounded in decades of experience—were conceived in a categorical form, relying on discrete depth intervals and piezometric states. Their raw discretization does not capture the natural variability of field conditions, nor does it allow seamless integration with physically based or data-driven modeling workflows.

By defining appropriate linguistic variables, constructing membership functions, and implementing a Mamdani fuzzy inference system, this section builds a computational mechanism capable of:

1. interpreting the hydrogeological state of a given slope in terms of fuzzy expert concepts;
2. evaluating the expected effectiveness of each guideline;
3. producing a ranked, site-specific recommendation that simultaneously considers effectiveness and applicability constraints.

In intuitive terms, this section describes how qualitative expert judgments are systematically translated into a quantitative and tailored decision-making tool to support the prioritization of mitigation measures.

3.1 Definition of linguistic variables and membership functions

Two hydrogeologically relevant variables were used as input:

- the depth of the sliding surface z_s;
- the final piezometric level z_w^{final}.

These two parameters were selected, according to Deliverable 3.3, as they are among the main factors that control both the mechanical behavior of a potentially unstable slope and the hydrological forcing that may trigger a landslide. From a geotechnical perspective, the depth of the sliding surface determines the geometry of the failure mechanism, the mobilized soil mass, and the stress distribution along the shear plane. Shallow instabilities typically respond rapidly to rainfall-induced infiltration, whereas deeper sliding surfaces involve larger volumes, slower hydrological response times, and different categories of countermeasures. For this reason, expert-based guideline tables traditionally distinguish mitigation strategies based on discrete depth intervals, reflecting established empirical and analytical knowledge about slope stability processes.

On the other hand, the final piezometric level z_w^{final} provides a direct measure of the subsurface water pressure conditions, which is one of the most influential driving forces in slope failure. Rising groundwater levels reduce effective stresses, modify shear strength parameters, and generate seepage forces that can destabilize the soil mass. Therefore, high piezometric conditions are strongly correlated with increased landslide susceptibility. Because many mitigation measures—such as drainage systems or water table control

Funded by the European Union. Views and opinions expressed are however those of the author(s) only and do not necessarily reflect those of the European Union. Neither the European Union nor the granting authority can be held responsible for them.

strategies—derive their effectiveness from how they alter pore-water pressure, the piezometric variable naturally forms the second axis of the expert knowledge structure.

For these reasons, using z_s and z_w^{final} as input variables allows the fuzzy inference system to replicate, formalize, and extend the reasoning embedded in expert guideline matrices. Their continuous nature makes them particularly suitable for representation through overlapping fuzzy sets, enabling smooth transitions between classes and more accurate modeling of intermediate hydrogeological states.

3.1.1 Depth of the sliding surface (z_s)

The depth of the sliding surface can reasonably be defined in the continuous range $[0, 20]$ m. This interval covers the typical variation from shallow to moderately deep landslides (see Deliverables 3.2 and 3.2).

This universe of discourse was partitioned into five fuzzy sets: *superficial*, *shallow*, *medium*, *deep*, and *very deep*. Triangular membership functions were selected for their simplicity, interpretability, and ability to approximate gradual transitions between depth classes.

The core positions were chosen based on geotechnical domain knowledge:

- 0–1 m corresponds to *superficial* slides;
- 1–3 m corresponds to *shallow* slides;
- 3–8 m corresponds to *medium-depth* slides;
- 8–15 m corresponds to *deep* slides;
- 15–20 m corresponds to *very deep* slides.

The overlapping of the membership functions ensures that no sharp discontinuities occur, and that intermediate depths correctly activate more than one linguistic term in varying degrees.

3.1.2 Piezometric level (z_w^{final})

The piezometric level, within the range $[0, 4]$, was divided into the terms as follows: *absent*, *low*, and *high*. These categories respectively reflect typical hydrogeological scenarios: absence of pore pressure; moderate pore pressure; significant water table rise.

Because piezometric responses in slopes may be non-linear and site-dependent, overlapping membership functions were used to capture transitional states, for example, the distinction between "low" and "high" piezometric conditions is not strictly binary.

3.1.3 Effectiveness of mitigation measures

The output variable, Eff, describes the expected effectiveness of a guideline on a scale from 0 to 1. Four fuzzy sets were defined: *low*, *medium*, *high*, and *very high*. The adopted shapes (triangular functions) ensure both interpretability and ease of defuzzification.

Funded by the European Union. Views and opinions expressed are however those of the author(s) only and do not necessarily reflect those of the European Union. Neither the European Union nor the granting authority can be held responsible for them.

This fuzzy output allows the model to capture expert assessments in a continuous manner rather than imposing discrete categories. As such, guidelines that lie between two discrete effectiveness levels in expert tables can be represented smoothly.

3.2 Construction of the fuzzy rule base

Expert-derived tables report the expected effectiveness of each guideline for specific combinations of depth conditions and piezometric levels. These tables contain numerical entries in the set:

$$\{0,\ 0.25,\ 0.5,\ 1.0\},$$

each representing an approximate level of anticipated performance.

These numerical values were translated into linguistic terms, as shown in Table 2. This mapping enables the direct conversion of expert tables into a structured fuzzy rule base.

Tab. 2
Mapping between crisp matrix values and linguistic effectiveness terms.

Crisp value	Linguistic term	Interpretation
0.00	`low`	Ineffective or negligible impact
0.25	`medium`	Moderate effectiveness in favourable conditions
0.50	`high`	Generally effective
1.00	`very high`	Strong effectiveness across conditions

Each entry in the expert matrix contributes a rule of the form:

$$\text{IF } z_s \text{ is } D_i \text{ AND } z_w^{final} \text{ is } P_j \text{ THEN } Eff \text{ is } L_k.$$

Thus, for each guideline, a total of $5 \times 3 = 15$ rules were generated.

The full rule base respects:

- the hierarchical structure of depth and piezometric categories,
- expert evaluations extracted from technical guidelines,
- the need for smooth transitions in intermediate conditions.

3.3 Inference and defuzzification

The Mamdani inference system was implemented using:

- the **minimum** operator (min) for the logical AND;
- the **maximum** operator (max) for aggregation of rule outputs;

Funded by the European Union. Views and opinions expressed are however those of the author(s) only and do not necessarily reflect those of the European Union. Neither the European Union nor the granting authority can be held responsible for them.

- clipped implication applied to output membership functions.

This choice ensures that the combined fuzzy output remains interpretable and consistent with engineering intuition.

After aggregation, the resulting fuzzy effectiveness distribution is defuzzified. The centroid (center of area) method was chosen:

$$Eff^* = \frac{\int_0^1 x\,\mu_{Eff}(x)\,dx}{\int_0^1 \mu_{Eff}(x)\,dx}.$$

This method is widely recognized as the most reliable for engineering decision systems as it preserves the balance between all possible outcomes, rather than favoring extreme values.

3.4 Integration of effectiveness and applicability

Although fuzzy effectiveness captures technical performance, real-world decision-making must also consider the *applicability* of mitigation measures—whether a guideline is feasible, cost-effective and suitable for the specific site.

The applicability scores provided by experts were normalized as follows:

$$App_{norm}(i) = \frac{App(i)}{\max_j App(j)}.$$

The final decision metric is a weighted combination:

$$Score(i) = \alpha\, Eff^*(i) + (1-\alpha)\, App_{norm}(i),$$

with $\alpha = 0.7$ giving greater emphasis to technical effectiveness while still considering feasibility.

This formulation balances:

- the objective, model-driven evaluation of performance (via fuzzy logic);
- the expert-driven evaluation of practical implementability (via applicability).

3.5 Final ranking and selection of the optimal guideline

The following steps yield the final recommended guideline:

1. The crisp input values z_s and z_w^{final} are fuzzified into overlapping membership grades.
2. For each guideline, all relevant fuzzy rules are activated with the strengths determined by the fuzzified inputs.
3. The rules are aggregated and defuzzified into a single effectiveness score Eff^*.
4. Applicability values are normalized and combined with effectiveness via the multi-criteria score.

Funded by the European Union. Views and opinions expressed are however those of the author(s) only and do not necessarily reflect those of the European Union. Neither the European Union nor the granting authority can be held responsible for them.

5. Guidelines are sorted in descending order of $Score(i)$.

The highest-scoring guideline is interpreted as the most suitable countermeasure under the examined hydrogeological conditions.

This fuzzy-based ranking system offers the advantages as follows:

- it converts qualitative expert knowledge into a reproducible quantitative framework;
- it handles uncertainty and overlapping categories inherently present in slope behavior;
- it provides transparent and interpretable decision-making steps;
- it can adapt to updated expert tables or new input variables with minimal modification.

As a result, the proposed approach constitutes a robust, flexible, and scientifically grounded method for selecting mitigation guidelines in complex hydrogeological scenarios.

4. Example of Fuzzy-based guideline selection

To illustrate the fuzzy decision-support system described in the previous sections, we present a complete example based on a representative unstable slope. The purpose of this example is to show, step by step, how crisp inputs produced by the AI-based predictive models (i.e., the estimated depth of the sliding surface and the final piezometric level) are processed by the fuzzy inference engine, how guideline-specific effectiveness values are computed, and finally how these values are combined with applicability scores to obtain a ranked list of recommended countermeasures.

4.1 Input conditions

Assume the AI models estimated the following hydrogeological conditions:

$$z_s = 8.5 \text{ m}, \qquad z_w^{\text{final}} = 3.$$

These values represent a *deep sliding surface* and a *high piezometric level*. Both variables lie in transition zones between multiple linguistic classes defined in Section 3, making the case particularly suited to fuzzy inference. Unlike a crisp classification scheme, which would sharply assign these values to a single category, the fuzzy system accounts for intermediate conditions by assigning simultaneous, graded memberships.

4.1.1 Step 1: Fuzzification of the inputs

The depth value $z_s = 8.5$ m falls at the transition between the *deep* (3–15 m) and *very deep* (15–20 m) categories. Using the triangular membership functions defined earlier, the corresponding degrees of membership are:

$$\mu_{\text{deep}}(8.5) = 0.80, \qquad \mu_{\text{verydeep}}(8.5) = 0.00.$$

Funded by the European Union. Views and opinions expressed are however those of the author(s) only and do not necessarily reflect those of the European Union. Neither the European Union nor the granting authority can be held responsible for them.

Thus, the input condition is almost entirely characterized as a deep-seated slide, with negligible membership in the very-deep domain.

Similarly, the piezometric level $z_w^{\text{final}} = 3$ predominantly activates the *high* fuzzy set, while still preserving minor membership in the *low* class:

$$\mu_{\text{high}}(3) \approx 0.73, \qquad \mu_{\text{low}}(3) \approx 0.08, \qquad \mu_{\text{absent}}(3) = 0.00.$$

Therefore, the fuzzy representation can capture the fact that the water table is substantially elevated, but still lies near the boundary between moderate and high pressure conditions.

4.1.2 Step 2: Activation of the Fuzzy rules

Each guideline is associated with an expert-derived matrix of effectiveness values. After fuzzification, all rules whose antecedents match the activated fuzzy sets are triggered. In the present case, the following rules are activated with the highest intensity:

$$\text{IF } (z_s \text{ is deep}) \wedge (z_w^{\text{final}} \text{ is high}) \Rightarrow \text{Effectiveness} = L_{DH},$$
$$\text{IF } (z_s \text{ is deep}) \wedge (z_w^{\text{final}} \text{ is low}) \Rightarrow \text{Effectiveness} = L_{DL}.$$

Additional rules involving weaker sets (e.g., combination with $\mu_{\text{low}}(3)$) also contribute, although with significantly lower firing strengths.

The firing strength of each rule is computed as follows:

$$\alpha_{ij} = \min\big(\mu_{\text{depth}}(z_s), \mu_{\text{piezometric}}(z_w^{\text{final}})\big).$$

In this example, the dominant rule is the *deep* $\wedge$ *high* combination, confirming the hydrogeological severity of the scenario.

4.1.3 Step 3: Aggregation and defuzzification

The output of each active rule is clipped and aggregated into a composite fuzzy set:

$$\mu_{\text{Eff}}(x) = \max_k \ \min(\alpha_k, \mu_{L_k}(x)).$$

Given the strong activation of the *deep–high* condition, the aggregated effectiveness distribution tends to emphasize the linguistic categories *high* and *very high* when present in the guideline matrix.

Centroid defuzzification is applied to obtain a crisp effectiveness value:

$$\text{Eff}^* = \frac{\int_0^1 x\, \mu_{\text{Eff}}(x)\, \mathrm{d}x}{\int_0^1 \mu_{\text{Eff}}(x)\, \mathrm{d}x}.$$

Guidelines that are designed to counteract high pore pressure in deep-seated movements typically yield the largest defuzzified scores.

Funded by the European Union. Views and opinions expressed are however those of the author(s) only and do not necessarily reflect those of the European Union. Neither the European Union nor the granting authority can be held responsible for them.

4.1.4 Step 4: Integration with applicability scores

The fuzzy-derived effectiveness is then combined with the guideline-specific applicability index:

$$\text{Score}(i) = 0.7\,\text{Eff}^*(i) + 0.3\,\text{App}_{\text{norm}}(i).$$

This weighted sum balances technical performance with practical feasibility.

For deep and highly saturated conditions, guidelines that are technically effective but challenging to implement may still receive lower final scores than more feasible alternatives with only slightly lower effectiveness.

4.1.5 Step 5: Final ranking

Sorting the final scores in descending order yields a prioritized list of recommended measures. For the input conditions considered here ($z_s = 8.5$ m and $z_w^{\text{final}} = 3$), the system tends to favor guidelines specifically targeted at addressing deep failures coupled with elevated groundwater pressures. Depending on the guideline group (G1–G5), higher-ranked measures often include:

- deep drainage systems (vertical drains, sub-horizontal drains),
- reduction of pore-water pressure through relief wells,
- toe buttressing or stabilization fills,
- structural reinforcements (retaining walls, piles, micropiles),
- load reduction and regrading of the upslope area.

These results align with expert consensus: when the water table is significantly elevated and the sliding surface is deep, the most effective measures typically involve acting directly on pore-water pressure and resisting deep-seated shear deformation.

We showed this example to demonstrate how the fuzzy system synthesizes qualitative expert knowledge, quantitative hydrogeological predictions, and applicability constraints into a coherent, transparent, and reproducible decision-making process specifically tailored to severe slope instability conditions.

The following 3D plots represent the effectiveness surfaces of all measures defined in Deliverable 3.3, tailored based on the values of z_s and z_w^{final} obtained using the artificial intelligence core. Also, histograms show the rank of sub-guidelines for each group (see Deliverable 3.3), based on the combined fuzzy effectiveness score and applicability index.

Funded by the European Union. Views and opinions expressed are however those of the author(s) only and do not necessarily reflect those of the European Union. Neither the European Union nor the granting authority can be held responsible for them.

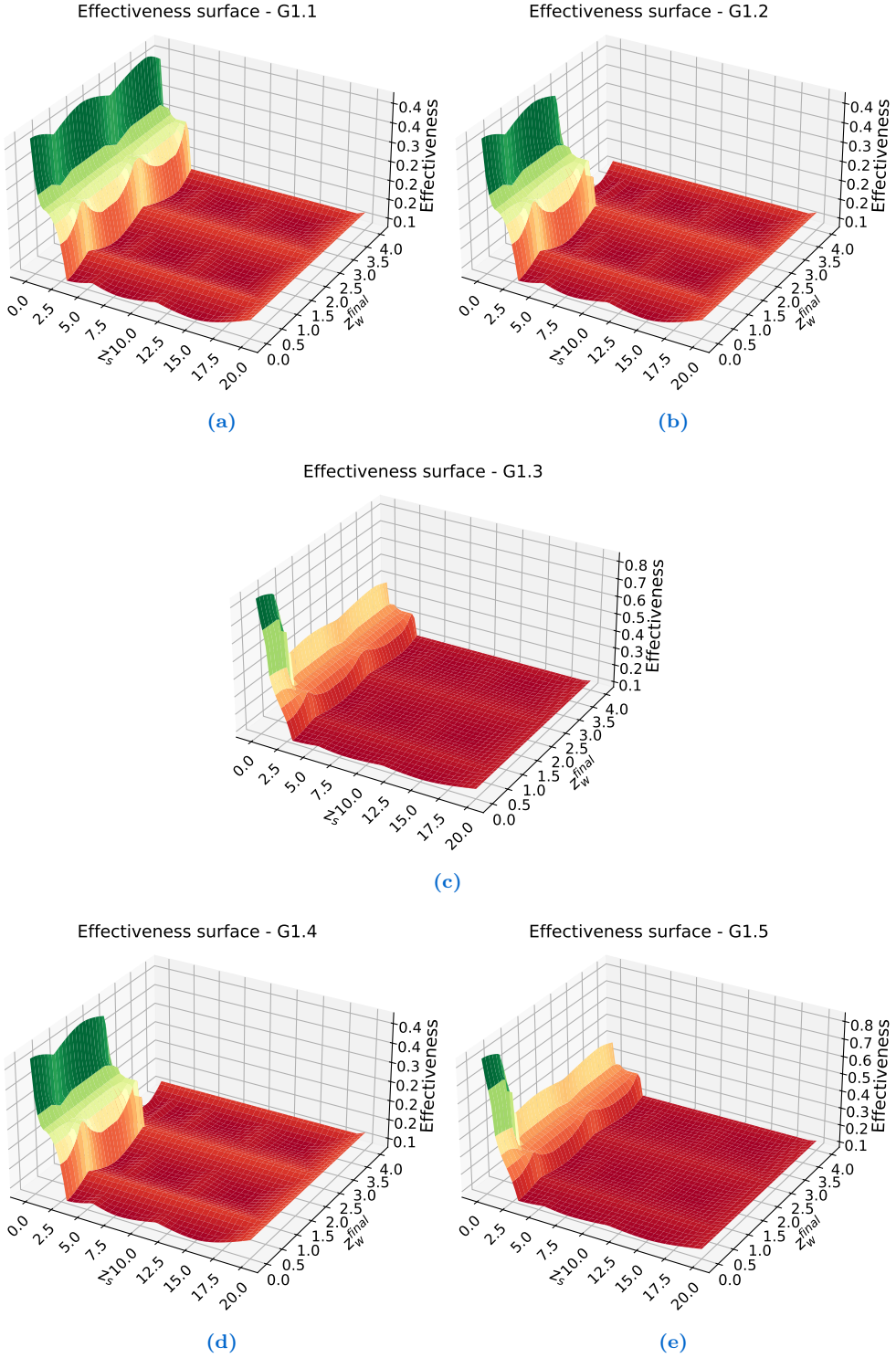

Fig. 2: Effectiveness surfaces obtained for the five sub-guidelines of Group 1 (G1.1–G1.5). Each 3D surface represents the fuzzy-inferred effectiveness as a function of the depth of the sliding surface (z_s) and the final piezometric level (z_w^{final}). Panels (a)–(e) correspond respectively to G1.1, G1.2, G1.3, G1.4, and G1.5. The colour gradient reflects increasing guideline effectiveness (from red = low to green = high), providing an interpretable mapping between hydrogeotechnical conditions and expert-based guideline performance.

Funded by the European Union. Views and opinions expressed are however those of the author(s) only and do not necessarily reflect those of the European Union. Neither the European Union nor the granting authority can be held responsible for them.

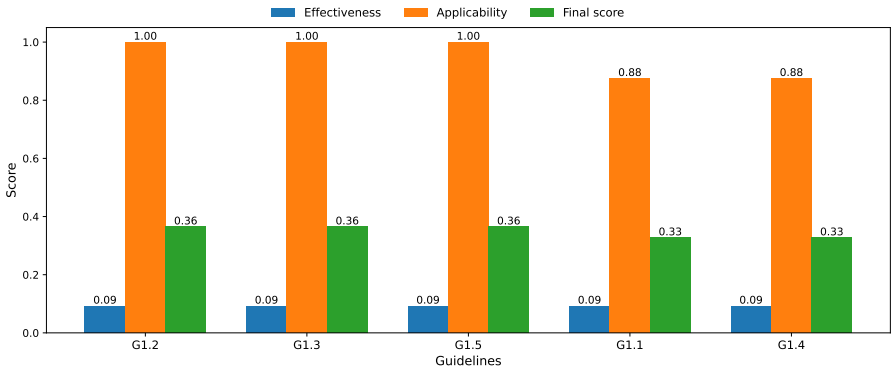

Fig. 3: Ranking of Group 1 sub-guidelines based on the combined fuzzy effectiveness score and applicability index. For each guideline, the bar plot reports: (i) the fuzzy-derived effectiveness for the selected state ($z_s = 2$ m, $z_w^{final} = 1$), (ii) the normalised applicability score derived from expert evaluation, (iii) the final weighted score used for guideline prioritisation. This representation highlights the trade-off between hydraulic–geotechnical effectiveness and real-world feasibility in the decision-making process.

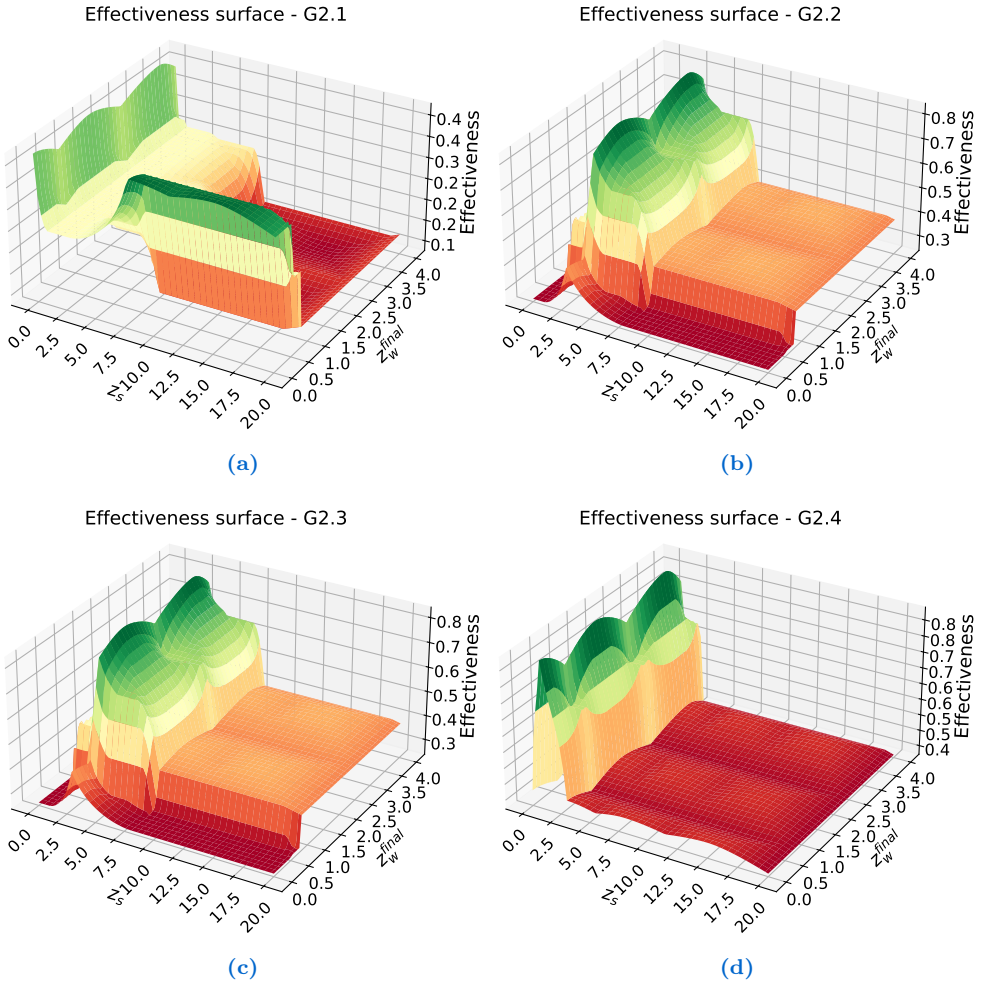

Fig. 4: Effectiveness surfaces obtained for the four sub-guidelines of Group 2 (G2.1–G2.4). Each 3D surface represents the fuzzy-inferred effectiveness as a function of the depth of the sliding surface (z_s) and the final piezometric level (z_w^{final}). Panels (a)–(d) correspond respectively to G2.1, G2.2, G2.3, G2.4. The colour gradient reflects increasing guideline effectiveness (from red = low to green = high), providing an interpretable mapping between hydrogeotechnical conditions and expert-based guideline performance.

Funded by the European Union. Views and opinions expressed are however those of the author(s) only and do not necessarily reflect those of the European Union. Neither the European Union nor the granting authority can be held responsible for them.

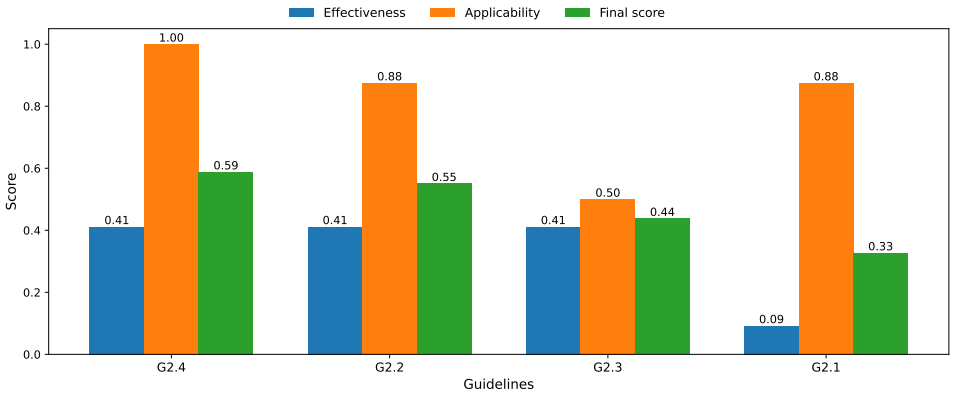

Fig. 5: Ranking of Group 2 sub-guidelines based on the combined fuzzy effectiveness score and applicability index. For each guideline, the bar plot reports: (i) the fuzzy-derived effectiveness for the selected state ($z_s = 2$ m, $z_w^{final} = 1$), (ii) the normalised applicability score derived from expert evaluation, (iii) the final weighted score used for guideline prioritisation. This representation highlights the trade-off between hydraulic–geotechnical effectiveness and real-world feasibility in the decision-making process.

Funded by the European Union. Views and opinions expressed are however those of the author(s) only and do not necessarily reflect those of the European Union. Neither the European Union nor the granting authority can be held responsible for them.

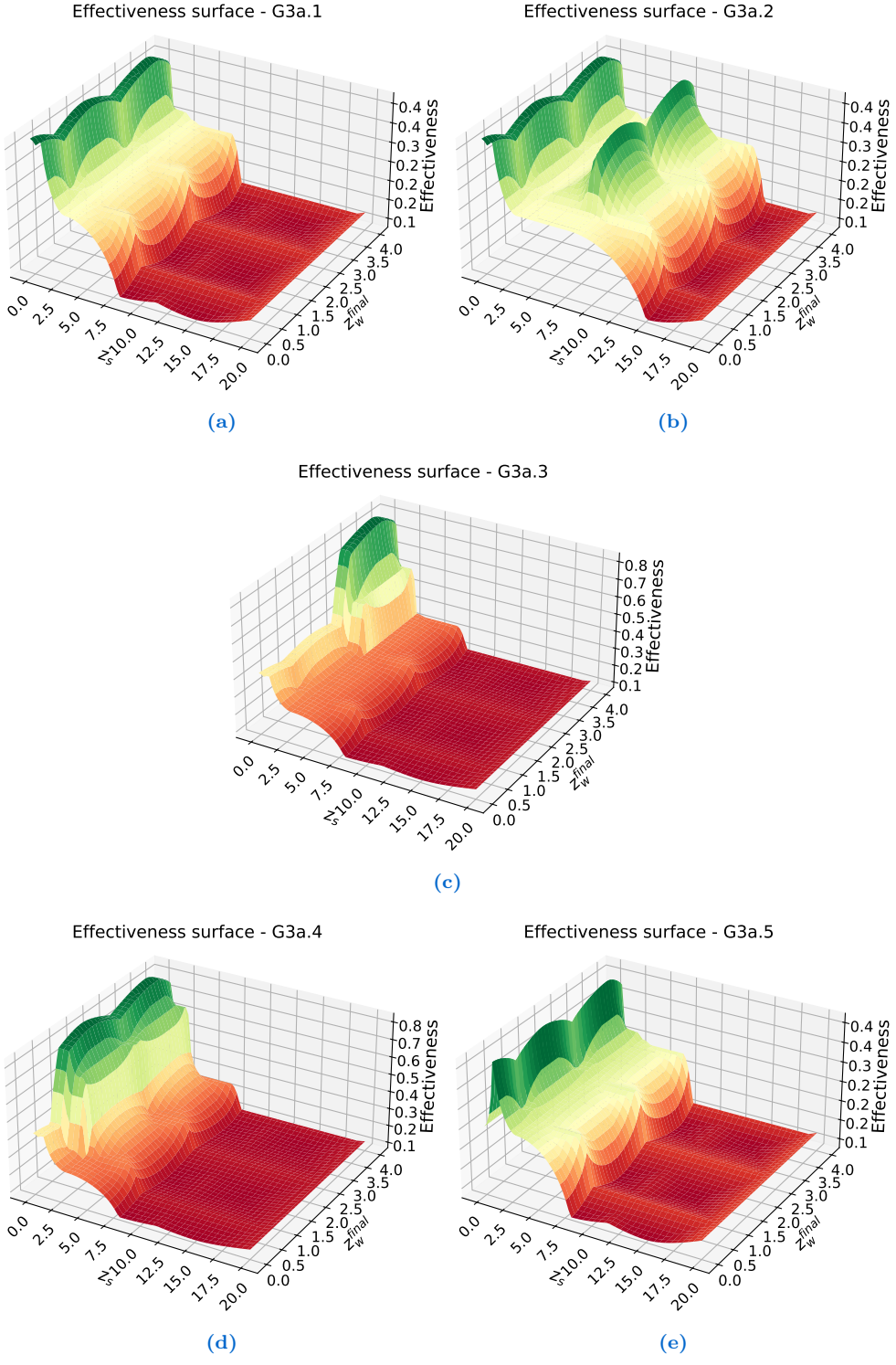

Fig. 6: Effectiveness surfaces obtained for the five sub-guidelines of Group 3a (G3a.1–G3a.5). Each 3D surface represents the fuzzy-inferred effectiveness as a function of the depth of the sliding surface (z_s) and the final piezometric level (z_w^{final}). Panels (a)–(e) correspond respectively to G3a.1, G3a.2, G3a.3, G3a.4, G3a.5. The colour gradient reflects increasing guideline effectiveness (from red = low to green = high), providing an interpretable mapping between hydrogeotechnical conditions and expert-based guideline performance.

Funded by the European Union. Views and opinions expressed are however those of the author(s) only and do not necessarily reflect those of the European Union. Neither the European Union nor the granting authority can be held responsible for them.

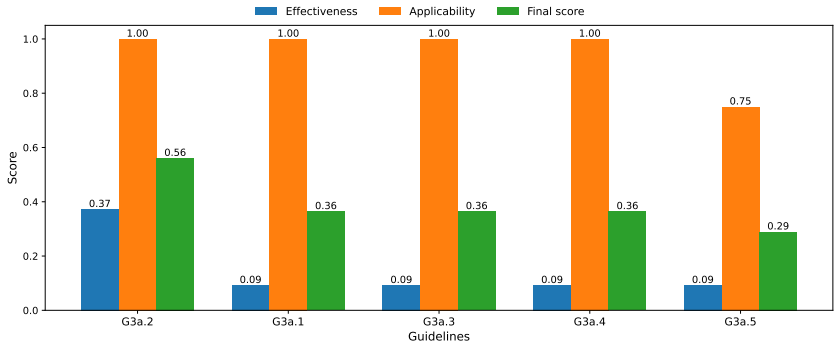

Fig. 7: Ranking of Group 3a sub-guidelines based on the combined fuzzy effectiveness score and applicability index. For each guideline, the bar plot reports: (i) the fuzzy-derived effectiveness for the selected state ($z_s = 2$ m, $z_w^{final} = 1$), (ii) the normalised applicability score derived from expert evaluation, (iii) the final weighted score used for guideline prioritisation. This representation highlights the trade-off between hydraulic–geotechnical effectiveness and real-world feasibility in the decision-making process.

Funded by the European Union. Views and opinions expressed are however those of the author(s) only and do not necessarily reflect those of the European Union. Neither the European Union nor the granting authority can be held responsible for them.

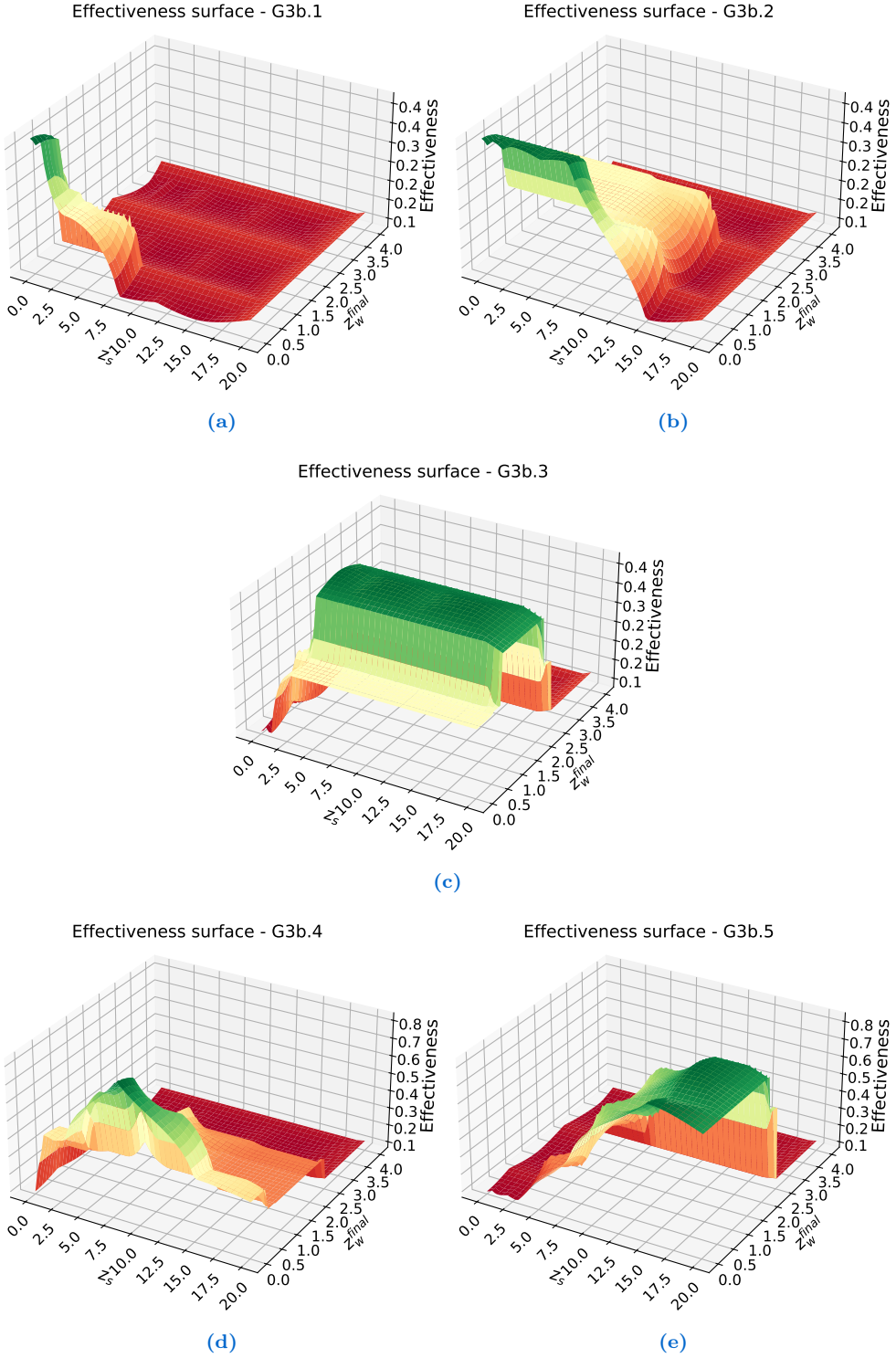

Fig. 8: Effectiveness surfaces obtained for the five sub-guidelines of Group 3b (G3b.1–G3b.5). Each 3D surface represents the fuzzy-inferred effectiveness as a function of the depth of the sliding surface (z_s) and the final piezometric level (z_w^{final}). Panels (a)–(e) correspond respectively to G3b.1, G3b.2, G3b.3, G3b.4, G3b.5. The colour gradient reflects increasing guideline effectiveness (from red = low to green = high), providing an interpretable mapping between hydrogeotechnical conditions and expert-based guideline performance.

Funded by the European Union. Views and opinions expressed are however those of the author(s) only and do not necessarily reflect those of the European Union. Neither the European Union nor the granting authority can be held responsible for them.

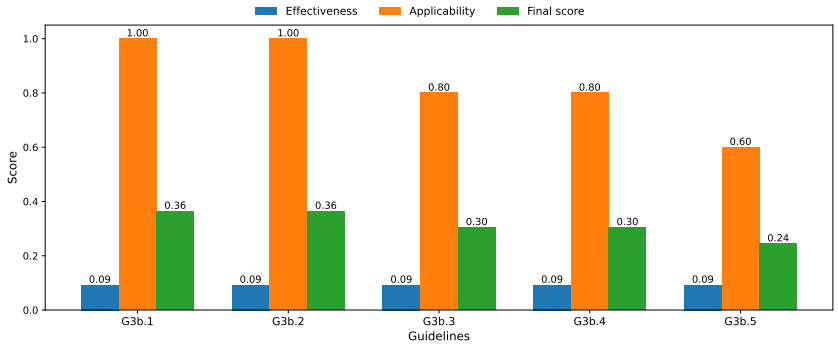

Fig. 9: Ranking of Group 3b sub-guidelines based on the combined fuzzy effectiveness score and applicability index. For each guideline, the bar plot reports: (i) the fuzzy-derived effectiveness for the selected state ($z_s = 2$ m, $z_w^{final} = 1$), (ii) the normalised applicability score derived from expert evaluation, (iii) the final weighted score used for guideline prioritisation. This representation highlights the trade-off between hydraulic–geotechnical effectiveness and real-world feasibility in the decision-making process.

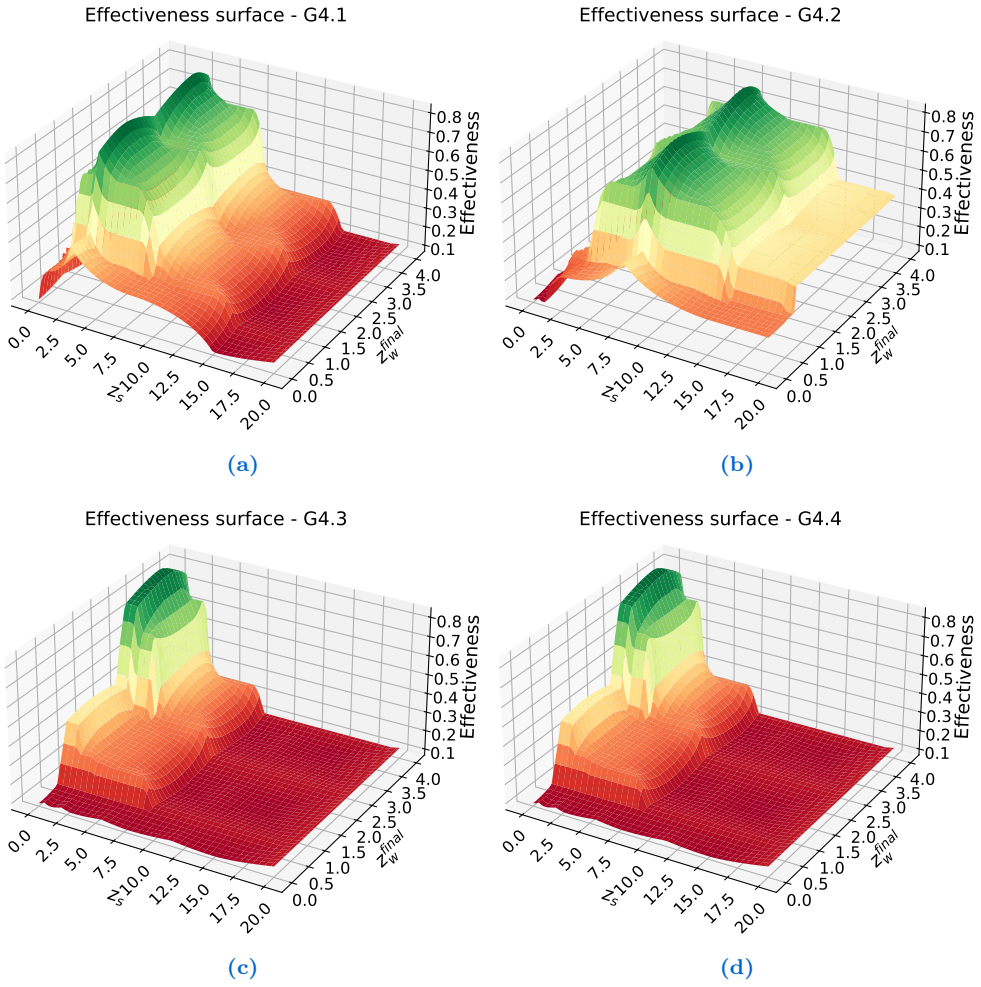

Fig. 10: Effectiveness surfaces obtained for the four sub-guidelines of Group 4 (G4.1–G4.4). Each 3D surface represents the fuzzy-inferred effectiveness as a function of the depth of the sliding surface (z_s) and the final piezometric level (z_w^{final}). Panels (a)–(d) correspond respectively to G4.1, G4.2, G4.3, G4.4. The colour gradient reflects increasing guideline effectiveness (from red = low to green = high), providing an interpretable mapping between hydrogeotechnical conditions and expert-based guideline performance.

Funded by the European Union. Views and opinions expressed are however those of the author(s) only and do not necessarily reflect those of the European Union. Neither the European Union nor the granting authority can be held responsible for them.

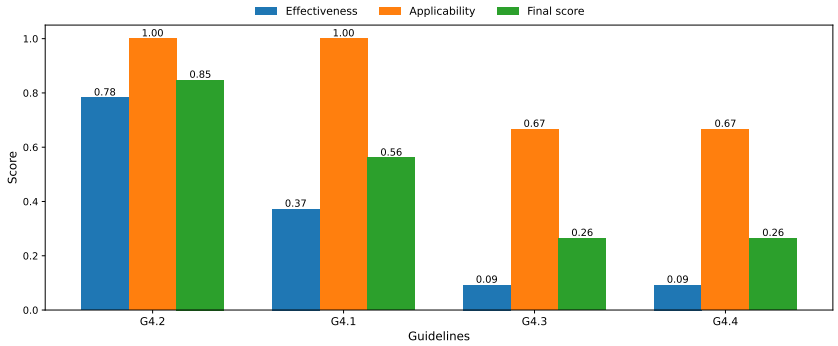

Fig. 11: Ranking of Group 4 sub-guidelines based on the combined fuzzy effectiveness score and applicability index. For each guideline, the bar plot reports: (i) the fuzzy-derived effectiveness for the selected state ($z_s = 2$ m, $z_w^{final} = 1$), (ii) the normalised applicability score derived from expert evaluation, (iii) the final weighted score used for guideline prioritisation. This representation highlights the trade-off between hydraulic–geotechnical effectiveness and real-world feasibility in the decision-making process.

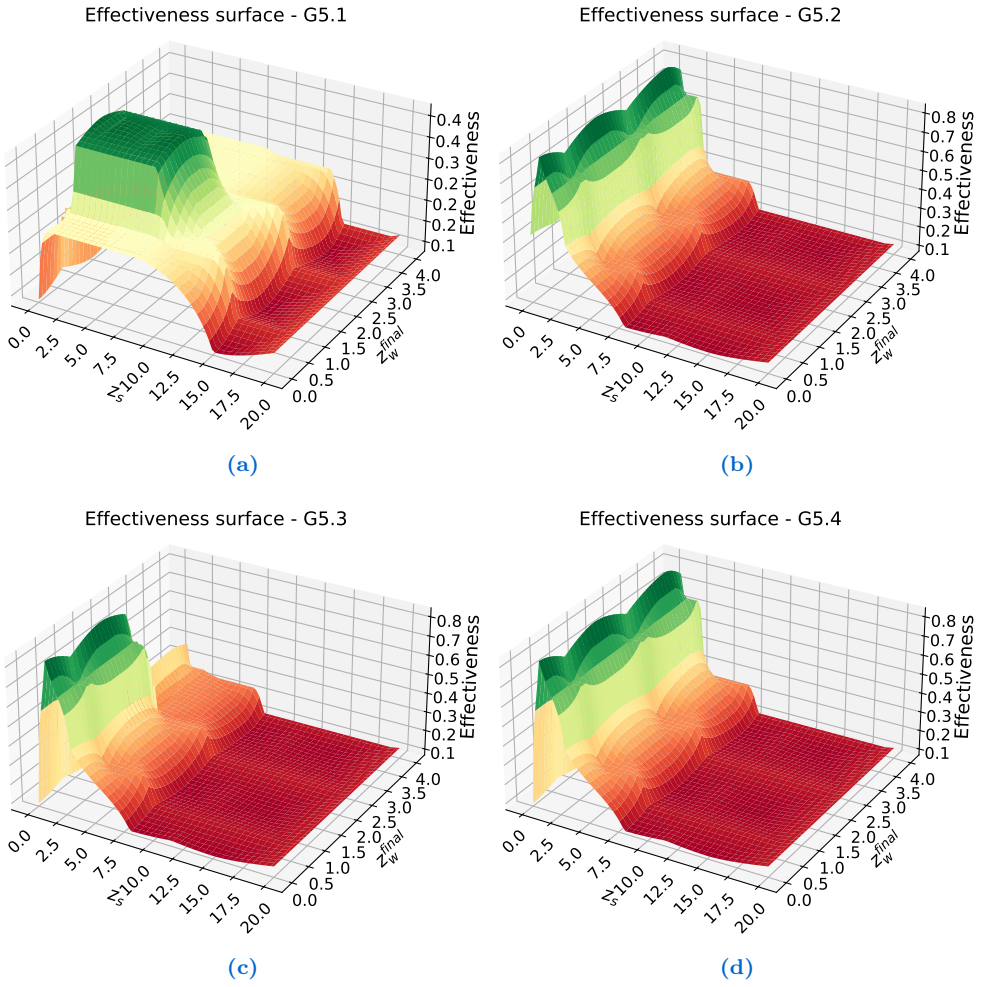

Fig. 12: Effectiveness surfaces obtained for the five sub-guidelines of Group 5 (G5.1–G5.4). Each 3D surface represents the fuzzy-inferred effectiveness as a function of the depth of the sliding surface (z_s) and the final piezometric level (z_w^{final}). Panels (a)–(e) correspond respectively to G5.1, G5.2, G5.3, G5.4, and G5.5. The colour gradient reflects increasing guideline effectiveness (from red = low to green = high), providing an interpretable mapping between hydrogeotechnical conditions and expert-based guideline performance.

Funded by the European Union. Views and opinions expressed are however those of the author(s) only and do not necessarily reflect those of the European Union. Neither the European Union nor the granting authority can be held responsible for them.

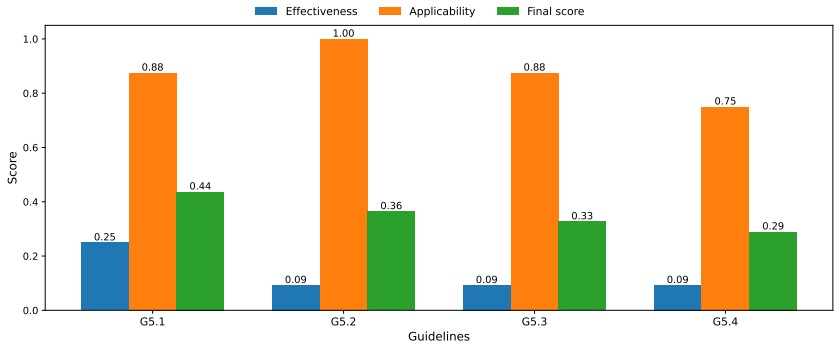

Fig. 13: Ranking of Group 5 sub-guidelines based on the combined fuzzy effectiveness score and applicability index. For each guideline, the bar plot reports: (i) the fuzzy-derived effectiveness for the selected state ($z_s = 2$ m, $z_w^{final} = 1$), (ii) the normalised applicability score derived from expert evaluation, (iii) the final weighted score used for guideline prioritisation. This representation highlights the trade-off between hydraulic–geotechnical effectiveness and real-world feasibility in the decision-making process.

Funded by the European Union. Views and opinions expressed are however those of the author(s) only and do not necessarily reflect those of the European Union. Neither the European Union nor the granting authority can be held responsible for them.

5. Hydraulic hazard assessment and guideline selection

The SAFE-LAND decision-support system integrates a complementary *hydraulic module* aimed at evaluating the hazards induced by flooding, channel overtopping, and rapid surface water propagation. This component is essential because many slope failures, debris flows, and shallow landslides are hydraulically triggered or exacerbated by high-intensity rainfall events and runoff concentration. For this reason, the hydraulic analysis is designed to operate in parallel with the fuzzy logic model, providing additional guideline recommendations specifically targeted at reducing water-related impacts.

The hydraulic module relies on three physically meaningful variables produced by the numerical simulations:

1. arrival time of the water front;
2. maximum water depth;
3. flow velocity.

These variables jointly describe the intensity of the hydraulic forcing and the velocity and erosive potential of the flow.

A semantic segmentation model classifies each pixel of the simulation domain into discrete hazard classes corresponding to different levels of hydraulic intensity. The resulting segmented maps form the basis for the automatic selection of hydraulic mitigation guidelines.

5.1 Hydraulic input variables and semantic segmentation

Three raster layers are generated from the hydraulic simulation:

1. **Water depth** $h(x, y)$, expressed in meters, representing the maximum water level attained during the event.
2. **Arrival time** $t_{\text{arr}}(x, y)$, indicating when the flowing water first reaches each grid cell.
3. **Flow velocity** $v(x, y)$, describing the peak flow speed, which correlates strongly with erosive power and transport capacity.

Each layer is processed through a dedicated segmentation model trained to distinguish areas of distinct hydraulic relevance. The classifier assigns every pixel to one of four hazard classes:

$$\{\text{green},\ \text{yellow},\ \text{orange},\ \text{red}\},$$

corresponding respectively to *low*, *moderate*, *substantial*, and *critical* hydraulic hazard. The colour-coded representation allows visual interpretation while enabling quantitative analysis for guideline selection.

Funded by the European Union. Views and opinions expressed are however those of the author(s) only and do not necessarily reflect those of the European Union. Neither the European Union nor the granting authority can be held responsible for them.

5.1.1 Green areas

Green pixels correspond to minimal hydraulic impact. They are characterized by shallow water depth (typically below a few centimetres), long arrival times, and negligible velocities. In these areas, water propagation is diffuse and slow, and no significant erosive or structural threat is expected. Hydraulic guidelines are generally not required or limited to basic drainage maintenance.

5.1.2 Yellow areas

Yellow segments are areas of moderate hazard, where water depth increases sufficiently to generate localized ponding or shallow overland flow. Arrival times may remain relatively high, indicating slow propagation, but flow velocities show noticeable increments. These zones may start to exert lateral pressure on structures or generate limited sediment transport. Hydraulic guidelines focus on redirecting diffuse flow, reducing local water accumulation, and preventing incipient erosion.

5.1.3 Orange areas

Orange areas denote substantial hydraulic impact. Here, depths are greater, arrival times are shorter (indicating rapid onset), and velocities reach values capable of mobilizing loose sediment and interacting dynamically with the terrain. Such behaviour is typical of flash-flood-prone zones or drainage pathways experiencing channelized flow. Mitigation guidelines in orange zones aim at intercepting, slowing, or safely conveying large water volumes before they accumulate hazardous momentum.

5.1.4 Red areas

Red pixels represent critical hydraulic hazard, defined by deep, fast, and rapidly arriving flows. These are the regions where peak discharges exhibit both destructive energy and erosive capacity. In the context of slope stability, red areas are strongly correlated with shallow debris flows, gully erosion, embankment overtopping, or severe runoff concentration. Interventions must therefore be robust, structural, and designed to withstand high hydraulic loads.

6. Modulated flood-risk assessment

This section presents the formulation of the proposed risk-assessment framework. The objective is to preserve the regulatory risk class R_{base} imposed by the EU Floods Directive while enriching it with a modulation coefficient $\alpha \in [0, 1]$ derived from hydrodynamic severity indicators computed at pixel level. The mathematical discussion highlights the functional properties of the indicators, the stability of the formulation, and the structural interpretation of α as a linear operator acting on spatial distributions of severity.

Funded by the European Union. Views and opinions expressed are however those of the author(s) only and do not necessarily reflect those of the European Union. Neither the European Union nor the granting authority can be held responsible for them.

6.1 Hydrodynamic representation on a discrete spatial domain

The basin $\Omega \subset \mathbb{R}^2$ is discretized into pixels $\mathcal{P} = \{p_1, \ldots, p_N\}$, with $N = |\mathcal{P}|$. For a hydrological event with return period T_r, simulation models produce three integer-valued hydrodynamic quantities at each pixel p:

$$A(p), H(p), V(p) \in \{1, 2, 3, 4\}, \tag{1}$$

representing the arrival time of the inundation front, the maximum water depth, and the maximum velocity, respectively. Although these values lie in a discrete set, they induce continuous modulation indicators through aggregation across Ω.

Each pixel is assigned to one of four severity classes via a mapping

$$\text{sev}(X(p)) \in \{\text{red, orange, yellow, green}\}, \quad X \in \{A, H, V\}, \tag{2}$$

determined by expert-informed thresholds. Let $N_{\text{red}}^{(X)}$, $N_{\text{orange}}^{(X)}$, $N_{\text{yellow}}^{(X)}$, and $N_{\text{green}}^{(X)}$ denote the number of pixels assigned to each class. Class contributions are weighted as follows:

$$w_{\text{red}} = 1, \qquad w_{\text{orange}} = 0.5, \qquad w_{\text{yellow}} = 0.25, \qquad w_{\text{green}} = 0.$$

6.2 Mathematical properties of the modulation indicators

The modulation indicator ρ_X is defined by

$$\rho_X = \frac{w_{\text{red}} N_{\text{red}}^{(X)} + w_{\text{orange}} N_{\text{orange}}^{(X)} + w_{\text{yellow}} N_{\text{yellow}}^{(X)} + w_{\text{green}} N_{\text{green}}^{(X)}}{N}. \tag{3}$$

This expression can be rewritten as an expectation:

$$\rho_X = \mathbb{E}_p\big[w\big(\text{sev}(X(p))\big)\big], \tag{4}$$

where the expectation is taken over the uniform distribution on $\mathcal{P}$. Several mathematical properties follow immediately:

Boundedness. Since $0 \le w(\cdot) \le 1$, one has $0 \le \rho_X \le 1$.

Convexity. If the severity distribution is modified by redistributing pixel weights across classes while maintaining the same total number of pixels, then ρ_X varies linearly in response. Thus, ρ_X is a convex functional on the simplex of class-proportion vectors.

Monotonicity. If the severity of any pixel is increased (e.g. green → yellow or yellow → orange), then ρ_X cannot decrease.

Lipschitz continuity. Let ρ_X and ρ'_X correspond to two distributions that differ by k pixels changing severity class. Then

$$|\rho_X - \rho'_X| \le \frac{k}{N}. \tag{5}$$

Thus the indicator is stable under small perturbations of pixel-level values.

Funded by the European Union. Views and opinions expressed are however those of the author(s) only and do not necessarily reflect those of the European Union. Neither the European Union nor the granting authority can be held responsible for them.

Interpretation as a linear functional. Let $p_{\text{red}}, p_{\text{orange}}, p_{\text{yellow}}, p_{\text{green}}$ denote the class proportions. Then

$$\rho_X = \langle p, w \rangle \tag{6}$$

where $p = (p_{\text{red}}, p_{\text{orange}}, p_{\text{yellow}}, p_{\text{green}})$ and $w = (1, 0.5, 0.25, 0)$. This clarifies that ρ_X is a linear operator acting on the severity-distribution vector.

These properties guarantee that the modulation indicators respond in a stable and interpretable manner to changes in the hydrodynamic field.

6.3 Regulatory risk and convex modulation

The regulatory component of the risk assessment is determined by the damage class $D \in \{D_1, D_2, D_3, D_4\}$ and hazard class $P \in \{P_1, P_2, P_3\}$ through the matrix $R_{\text{base}} = \mathcal{M}(D, P)$ (see Deliverable 3.2). The enhanced representation used to tailor guidelines relies on a modulation coefficient

$$\alpha = W_A(D)\,\rho_A + W_H(D)\,\rho_H + W_V(D)\,\rho_V, \tag{7}$$

where the nonnegative weights satisfy $W_A(D) + W_H(D) + W_V(D) = 1$. This choice has two main motivations. First, expressing α as a convex combination of the indicators ρ_A, ρ_H, ρ_V guarantees that $\alpha \in [0, 1]$ and that it can be interpreted as a normalized measure of hydrodynamic severity, consistent with the scale of the underlying indicators. Second, the explicit dependence of the weights on the damage class D allows the model to reflect that the relative importance of arrival time, depth, and velocity is not uniform across land uses: for example, fast and deep flows are more critical in densely urbanized or infrastructural areas than in natural or agricultural zones.

We specify the weights $W_A(D)$, $W_H(D)$, and $W_V(D)$ on the basis of the semantics of the damage classes D_1–D_4 described in Deliverable 3.2. The adopted values are

$$\begin{aligned}
D_1 \text{ (low damage)}: &\quad W_A = 0.20,\ W_H = 0.50,\ W_V = 0.30,\\
D_2 \text{ (moderate damage)}: &\quad W_A = 0.25,\ W_H = 0.45,\ W_V = 0.30,\\
D_3 \text{ (medium damage)}: &\quad W_A = 0.20,\ W_H = 0.40,\ W_V = 0.40,\\
D_4 \text{ (high damage)}: &\quad W_A = 0.15,\ W_H = 0.45,\ W_V = 0.40.
\end{aligned}$$

The structure of these weights is well-motivated. In all classes, the depth-related component ρ_H receives the largest share, reflecting the widely documented role of inundation depth as a primary driver of direct damage to buildings, contents, and productive assets. The velocity component ρ_V is assigned increasing relevance when moving from D_1 to D_3 and D_4. This is consistent with the interpretation of D_3 and D_4 as classes that contain infrastructure, industrial facilities, dense settlements, and critical services, where high-velocity flows exacerbate structural damage, erosion, and functional disruption. Conversely, the arrival-time component ρ_A plays a relatively larger role in the low- and moderate-damage classes D_1 and D_2, where longer warning times can significantly mitigate impacts, and a smaller role in D_4, where even with longer lead times the concentration of exposed values and strategic assets motivates a conservative treatment of depth and velocity.

Funded by the European Union. Views and opinions expressed are however those of the author(s) only and do not necessarily reflect those of the European Union. Neither the European Union nor the granting authority can be held responsible for them.

The weights can be configured and should be seen as an expert-informed parametrization that translates the qualitative descriptions of D_1–D_4 into a quantitative rule for combining the indicators. They preserve the ordering of *importance depth* > *velocity* > *arrival time* in all classes, while also allowing the relative contribution of each indicator to vary in a way that is coherent with the underlying land-use categories. In applications where empirical loss data are available, these values could be further refined or calibrated, but in the absence of such data they provide a transparent and interpretable baseline configuration.

Because α is a convex combination, $0 \leq \alpha \leq 1$. Additional properties include:

Monotonicity. If every ρ_X is increased (or remains unchanged), then α cannot decrease.

Sensitivity. If ρ_X changes by δ_X, then

$$\alpha' - \alpha = W_A(D)\,\delta_A + W_H(D)\,\delta_H + W_V(D)\,\delta_V.$$

Thus the effect of a perturbation is weighted by the relative importance of each indicator.

Lipschitz continuity. Since $W_A + W_H + W_V = 1$,

$$|\alpha' - \alpha| \leq \max\{|\delta_A|, |\delta_H|, |\delta_V|\}.$$

The final risk descriptor is the ordered pair $(R_{\text{base}}, \alpha)$, where R_{base} ensures regulatory compliance and α quantifies hydrodynamic severity.

6.4 Guideline selection

Each guideline g has an effectiveness $E(g) \in [0,1]$ and a normalized applicability $A(g) \in [0,1]$ (effectiveness and applicability are defined in Table 3.10 of Deliverable 3.3). With thresholds $0 \leq \tau_L < \tau_H \leq 1$, the selected guideline is

$$g^*(R_{\text{base}}, \alpha) = \begin{cases} \arg\max E(g), & \alpha \geq \tau_H, \\ \arg\max A(g), & \alpha \leq \tau_L, \\ \arg\max\big(\lambda(\alpha)E(g) + (1-\lambda(\alpha))A(g)\big), & \tau_L < \alpha < \tau_H, \end{cases} \tag{8}$$

where

$$\lambda(\alpha) = \frac{\alpha - \tau_L}{\tau_H - \tau_L}. \tag{9}$$

This rule formalizes the idea that the modulation coefficient α expresses the hydrodynamic intensity of the event and therefore acts as a continuous indicator of how demanding the mitigation or preparedness action should be. When α is small (i.e. $\alpha \leq \tau_L$), the simulated flood conditions are mild and the spatial distribution of severe pixels is limited; under these circumstances it is reasonable to prioritize measures that are easy to implement, readily achievable, and compatible with local constraints, hence the selection is driven entirely by the applicability score $A(g)$. Conversely, when α is large (i.e. $\alpha \geq \tau_H$), the hydrodynamic severity is pronounced and a significant portion of the basin experiences

Funded by the European Union. Views and opinions expressed are however those of the author(s) only and do not necessarily reflect those of the European Union. Neither the European Union nor the granting authority can be held responsible for them.

critical conditions. In this regime, priority must be given to the capacity of a measure to effectively reduce risk, and the choice is therefore governed by the effectiveness score $E(g)$ alone.

In the intermediate region $\tau_L < \alpha < \tau_H$, neither applicability nor effectiveness dominates in isolation. The factor $\lambda(\alpha)$ provides a smooth, monotone interpolation between the two extremes: it increases linearly from 0 at $\alpha = \tau_L$ to 1 at $\alpha = \tau_H$. As a result, when α is close to τ_L, the decision continues to favor applicability, whereas when α approaches τ_H, effectiveness progressively acquires greater influence. This construction ensures continuity of the decision rule with respect to α, avoiding sharp switches between guidelines and guaranteeing that the recommended action responds in a stable and interpretable way to changes in hydrodynamic conditions.

Overall, the pair $(R_{\text{base}}, \alpha)$ determines both the admissible set of guidelines (through the regulatory class R_{base}) and their prioritization (through the continuous modulation coefficient α). This separation of roles allows the method to remain fully compliant with the institutional risk classification while still providing a fine-grained and operationally meaningful mechanism to select the most appropriate guideline for a given flood scenario.

Funded by the European Union. Views and opinions expressed are however those of the author(s) only and do not necessarily reflect those of the European Union. Neither the European Union nor the granting authority can be held responsible for them.

6.5 Algorithm

Algorithm 1: Modulated Flood-Risk Assessment Procedure

Input: Basin domain Ω, pixel set $\mathcal{P}$, return period T_r.
Output: Regulatory risk class R_{base}, modulation coefficient α, selected guideline g^*.

AI inference
Run the AI model on the event with return period T_r to obtain, for all $p \in \mathcal{P}$, the quantities:
    arrival time $A(p)$, depth $H(p)$, velocity $V(p)$.
Severity Classification and Modulation Indicators
for $X \in \{A, H, V\}$ **do**
    For each pixel p, compute severity label $\text{sev}(X(p)) \in \{\text{red}, \text{orange}, \text{yellow}, \text{green}\}$.
    Count $N^{(X)}_{\text{red}}$, $N^{(X)}_{\text{orange}}$, $N^{(X)}_{\text{yellow}}$, $N^{(X)}_{\text{green}}$.
    Compute modulation indicator:

$$\rho_X = \frac{1 \cdot N^{(X)}_{\text{red}} + 0.5 \cdot N^{(X)}_{\text{orange}} + 0.25 \cdot N^{(X)}_{\text{yellow}}}{|\mathcal{P}|}.$$

end
Regulatory Classification
Determine damage class D from land use.
Assign hazard class P from the return period T_r.
Compute baseline regulatory risk

$$R_{\text{base}} = \mathcal{M}(D, P).$$

Risk Modulation
Retrieve the weights $(W_A(D), W_H(D), W_V(D))$ associated with D.
Compute

$$\alpha = W_A(D)\rho_A + W_H(D)\rho_H + W_V(D)\rho_V.$$

Guideline Selection
Select guideline g^* via

$$g^* = \begin{cases} \arg\max E(g), & \alpha \geq \tau_H, \\ \arg\max A(g), & \alpha \leq \tau_L, \\ \arg\max\big(\lambda(\alpha)E(g) + (1-\lambda(\alpha))A(g)\big), & \tau_L < \alpha < \tau_H, \end{cases}$$

with $\lambda(\alpha) = \dfrac{\alpha - \tau_L}{\tau_H - \tau_L}$.

return $(R_{\text{base}}, \alpha, g^*)$.

Funded by the European Union. Views and opinions expressed are however those of the author(s) only and do not necessarily reflect those of the European Union. Neither the European Union nor the granting authority can be held responsible for them.

The algorithm emphasizes that the regulatory classification and the modulation procedure are logically independent: the former depends solely on (D, P), whereas the latter incorporates hydrodynamic intensities. The flow diagram is as follows:

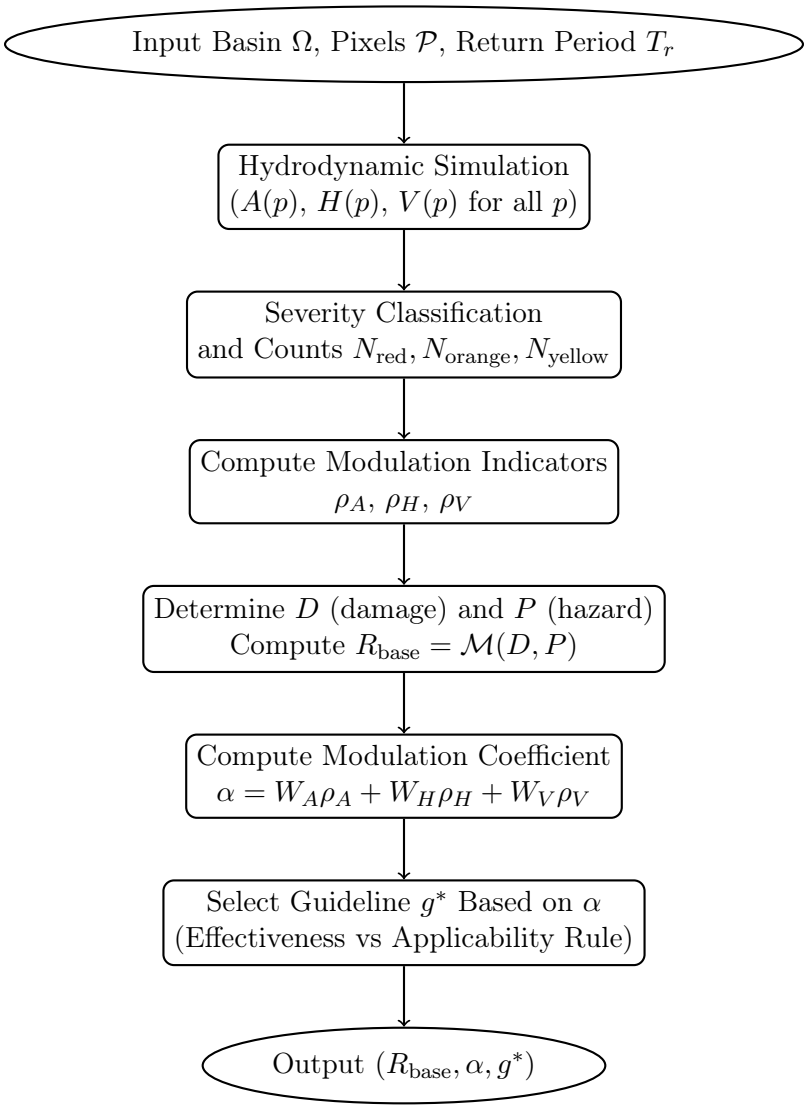

Fig. 14: Flow diagram of the modulated flood-risk assessment method. The regulatory risk class R_{base} is kept intact, while the hydrodynamic indicators contribute to the continuous modulation coefficient α, which guides the selection of the most appropriate guideline.

7. Example of modulated flood-risk assessment and guideline selection

This section illustrates the application of the modulated risk-assessment procedure using the segmented maps shown in Figure 15. The maps correspond to the arrival time, flow velocity, and water depth fields discretized into categorical hazard classes. The procedure follows the mathematical formulation described in the previous section and results in both the computation of the modulation coefficient α and the selection of the most appropriate guideline.

Funded by the European Union. Views and opinions expressed are however those of the author(s) only and do not necessarily reflect those of the European Union. Neither the European Union nor the granting authority can be held responsible for them.

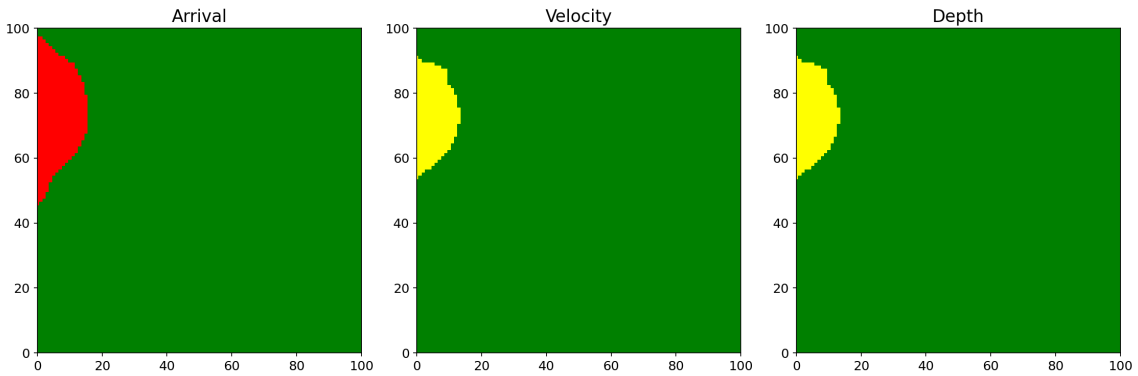

Fig. 15: Segmented maps generated by the system for hydraulic hazard assessment. The panels show, from left to right, the spatial distributions of arrival time, flow velocity, and water depth, discretized into qualitative hazard classes (green–yellow–orange–red). These maps are generated by the procedure described in Algorithm 1 in Section 6.5.

7.1 Extraction of severity indicators

The domain is discretized into $100 \times 100 = 10{,}000$ pixels. Each pixel is assigned a severity class from the set

$$\{\text{red}, \text{orange}, \text{yellow}, \text{green}\}.$$

Counting the pixels in each category from the segmented maps, we obtain the following values:

Arrival map:

$$N^{(A)}_{\text{red}} \approx 1800, \qquad N^{(A)}_{\text{yellow}} = 0, \qquad N^{(A)}_{\text{orange}} = 0, \qquad N^{(A)}_{\text{green}} \approx 8200.$$

The corresponding modulation indicator is

$$\rho_A = \frac{1 \cdot N^{(A)}_{\text{red}} + 0.5 \cdot N^{(A)}_{\text{orange}} + 0.25 \cdot N^{(A)}_{\text{yellow}}}{10{,}000} = 0.18.$$

Velocity map:

$$N^{(V)}_{\text{yellow}} \approx 750, \qquad N^{(V)}_{\text{orange}} = 0, \qquad N^{(V)}_{\text{red}} = 0.$$

Thus,

$$\rho_V = \frac{0.25 \cdot N^{(V)}_{\text{yellow}}}{10{,}000} = 0.01875.$$

Depth map:

$$N^{(H)}_{\text{yellow}} \approx 700, \qquad N^{(H)}_{\text{orange}} = 0, \qquad N^{(H)}_{\text{red}} = 0.$$

Thus,

$$\rho_H = \frac{0.25 \cdot N^{(H)}_{\text{yellow}}}{10{,}000} = 0.0175.$$

Funded by the European Union. Views and opinions expressed are however those of the author(s) only and do not necessarily reflect those of the European Union. Neither the European Union nor the granting authority can be held responsible for them.

7.2 Modulation coefficient

The modulation coefficient α is computed using the convex combination

$$\alpha = W_A(D)\,\rho_A + W_H(D)\,\rho_H + W_V(D)\,\rho_V.$$

Assuming a moderate damage class D_2, the corresponding weights are

$$W_A = 0.25, \qquad W_H = 0.45, \qquad W_V = 0.30.$$

Therefore,

$$\alpha = 0.25 \cdot 0.18 + 0.45 \cdot 0.0175 + 0.30 \cdot 0.01875 = 0.0593.$$

Since α is small, the hydrodynamic intensity is limited.

7.3 Guideline selection

Let the decision thresholds be

$$\tau_L = 0.10, \qquad \tau_H = 0.40.$$

The value of α satisfies

$$\alpha = 0.0593 < \tau_L,$$

and therefore the guideline is selected by maximizing applicability:

$$g^* = \arg\max A(g).$$

This corresponds to recommending measures that are easy to implement, compatible with the local terrain, and do not require heavy engineering. Typical examples include:

- reforestation and afforestation in watersheds;
- land use planning and zoning;
- urban green infrastructure;
- routine maintenance of watercourses, clearing and inspection of structures.

The risk descriptor obtained from this example is

$$(R_{\text{base}}, \alpha, g^*) = (R_{\text{base}}, 0.0593, g_{\text{applicable}}),$$

where R_{base} is the regulatory risk class determined by damage class and return period. The example shows that even in the presence of a sharp arrival front, shallow depths and low velocities yield a small modulation coefficient, leading to the selection of guidelines based on applicability rather than effectiveness. The procedure ensures compliance with regulatory constraints while providing actionable recommendations for local mitigation.

Funded by the European Union. Views and opinions expressed are however those of the author(s) only and do not necessarily reflect those of the European Union. Neither the European Union nor the granting authority can be held responsible for them.

8. Conclusions

This deliverable has developed an integrated and methodologically robust framework for tailoring hydrogeological mitigation guidelines through the combined use of artificial intelligence, fuzzy inference, and hydrodynamic modelling. The system does not merely assemble independent components: it builds a coherent decision-support system capable of translating heterogeneous geotechnical and hydraulic information into context-specific and operationally meaningful recommendations.

The fuzzy logic module demonstrates how expert knowledge (traditionally expressed through qualitative linguistic rules and categorical guideline tables) can be formalized into a continuous, explainable, and reproducible inference structure. By modeling key variables such as sliding-surface depth and piezometric level through overlapping linguistic sets, the system successfully captures the gradual transitions and uncertainties that characterize real slope behavior. The Mamdani-type inference mechanism yields effectiveness surfaces that evolve smoothly with changing conditions and allow nuanced comparisons between multiple guideline families. This alone represents a significant methodological advance as it provides a systematic means of preserving expert reasoning while enabling rigorous computational evaluation.

In parallel, hydraulic hazard assessment introduces an AI-supported stratification of flood severity using simulated arrival times, water depths, and flow velocities. Through semantic segmentation and pixel-level aggregation, the system identifies critical spatial patterns of hydraulic forcing. This enables guideline selection that is responsive to the magnitude of hydrodynamic stressors, but also to their spatial distribution and temporal onset. The subsequent modulation framework, grounded in interpretable severity indicators, further refines the risk description by coupling regulatory classifications with a continuous coefficient reflecting local flood intensity.

A major contribution of this part of the SAFE-LAND project is therefore the explicit integration of the geotechnical fuzzy system and the hydraulic hazard module into a unified decision-support architecture. This integration acknowledges that hydrogeological risk rarely arises from isolated mechanisms: landslides are frequently conditioned by subsurface saturation, while they are also triggered or intensified by surface runoff and flooding. By combining subsurface-oriented guidelines with surface-water mitigation measures, the framework supports truly multi-hazard reasoning and ensures that recommendations remain consistent across interacting processes.

Beyond methodological coherence, the proposed system is designed with operational applicability in mind. In particular, it provides transparent decision rules, traceable inference steps, and guideline rankings that can be easily interpreted by practitioners. In addition, the modularity of the framework allows it to be extended with updated expert tables, calibrated membership functions, enriched hydraulic variables, or additional data sources. The system is thus a crucial component of the SAFE-LAND project but also a flexible foundation for future advancements in AI-assisted hydrogeological risk management.

This deliverable consolidates expert knowledge, numerical simulation, machine learning, and explainable AI techniques into a scientifically sound and operationally comprehensive tool to select mitigation guidelines tailored to real environments. The methodology represents a significant step toward an integrated multi-layer platform for preventive

Funded by the European Union. Views and opinions expressed are however those of the author(s) only and do not necessarily reflect those of the European Union. Neither the European Union nor the granting authority can be held responsible for them.

planning, emergency response, and long-term land management in areas exposed to landslides and flood hazards.

Future refinements will focus on validation with the data from the case studies in the pilot areas, stakeholder engagement and refinement of the computational components to further strengthen the reliability and utility of the system in real-world decision-making.

Funded by the European Union. Views and opinions expressed are however those of the author(s) only and do not necessarily reflect those of the European Union. Neither the European Union nor the granting authority can be held responsible for them.